Vol 16 No 1, January 2007
1009-1963/2007/16(01)/0266-06

Chinese Physics

© 2007 Chin. Phys. Soc.
and IOP Publishing Ltd

Edge method for measuring source spot-size and its principle*

Shi Jiang-Jun(施将君), Liu Jun(刘 军), Liu Jin(刘 进)†, and Li Bi-Yong(李必勇)

Institute of Fluid Physics, China Academy of Engineering Physics, Mianyang 621900, *China*

(Received 16 February 2006; revised manuscript received 15 August 2006)

The edge method is used to measure the source spot-size. In this paper, the measuring principle and applying range are discussed. It is shown that the method can directly be used to measure the spot-size of either light source, or low-energy x-ray source, or x-ray source with an energy higher than 250 keV.

Keywords: edge method, edge spread function (ESF), linear spread function (LSF), full width at half maximum (FWHM)

PACC: 8170J

1. Introduction

It is appropriate to use transfer functions to characterize sources in optics. For example, the pinhole method is used to measure the source point spread function (PSF), the slit method can measure the source linear spread function, and the edge method can find the source linear spread function (LSF) from the edge spread function measured with the edge method.[1−3] The pinhole or slit cell is made of high-Z material with the thickness of a millimetre or less. These methods are the same as the measurements of the source spot size of x-ray with low energy.

The penetrability of high-energy x-ray is better than low-energy x-ray. For the high-energy x-ray, the results from the pinhole method and slit method are not in agreement with PSF and LSF of the source, so that these methods cannot directly measure the spot size of x-ray source with energy higher than 250 keV. But the edge method still can be used to measure the source spot size for the high-energy x-ray case. For a light, the edge cell is made of very thin screening materials. For the high-energy x-ray, it is made of high-Z material with thickness, h, of a few centimetres, so the image obtained shows clear contrast. The end side is parallel to the system axis. The x-rays across the end side will decay, and the exposure on the projecting zone of the end side of the edge cell will reduce. This paper mainly studies the effect of the thickness h on edge spread function (ESF) and LSF, and decides whether the edge method can directly measure the spot size of the high-energy x-ray source.

2. Theory

In cumulation emission of the axisymmetric x-ray source, the energy, transported from the source element $\mathrm{d}\xi\mathrm{d}\eta$ to unit area at point (x, y) on the imaging plane, is $\mathrm{d}I_i(x, y) = I_s(\xi, \eta)\mathrm{d}\xi\mathrm{d}\eta\mathrm{d}\vec{\Omega}$, where $I_s(\xi, \eta)$ is the normalized brightness distribution over the source area. So, the image intensity distribution is given by

$$I_i(x, y) = \frac{1}{2\pi d^2} \iint\limits_S I_s(\xi, \eta) T(u, v)\mathrm{d}\xi\mathrm{d}\eta, \qquad (1)$$

where (x, y), (ξ, η), and (u, v) are the corresponding transverse coordinates of the image plane, the source plane, and the middle plane of the edge cell, respectively. When the end side is on the system axis, the source point $(\xi_0(x), \eta_0(y))$ and the image point (x, y) are conjugated about the centre of end side of the edge cell, with

$$x = -M\xi_0(x), \quad y = -M\eta_0(y). \qquad (2)$$

In Eq.(1), $T(u, v)$ is the transmission function, and in Eq.(2) M is the magnification of the system. For the light and low-energy x-rays, the transmission function of the edge cell on the space $u \leq 0$ is expressed as the Heaviside unit function

$$T(u, v) = H(u). \qquad (3)$$

*Project supported by the foundation of China Academy of Engineering Physics (Grant No 025300).

†Corresponding author. E-mail: jnl0517@sina.com

For the high-energy x-ray, the edge cell transmission function is expressed as follows:

$$T(u,v) \approx \exp(-\tilde{\mu}\ell(x,\xi)), \tag{4}$$

where $\ell(x,\xi)$ is the path length of x-ray in the edge cell, and $\tilde{\mu}$ is the efficient linear attenuation coefficient of the edge cell. The length is approximately independent of the pixel coordinate y, when the radiographic distance d is larger enough than the thickness h and the geometric magnification M is not far from 1. The distances from the middle plane of the edge cell to the source plane and image plane are expressed by respectively parameters L_1 and L_2. So, $M = L_2/L_1$.

When the edge cell transmission function is the δ-function, $T(u,v) = \delta(u)$, the LSF of the source is written as

$$\mathrm{LSF}(x) = \frac{1}{2\pi d^2}\frac{m}{M}Y(\xi_0(x)), \tag{5}$$

where $m = M + 1$ and $Y(\xi)$ is the linear distribution function given by

$$Y(\xi) = \int_{-\eta(\xi)}^{\eta(\xi)} I_s(\xi,\eta)\mathrm{d}\eta. \tag{6}$$

For the axisymmetric source,

$$\eta(\xi_0(x)) = \sqrt{R_0^2 - \xi_0^2(x)},$$

where R_0 is the effective radius of the source.

3. The light case

From Eqs.(1) and (3), we obtain the ESF as

$$\begin{aligned}\mathrm{ESF}(x) &= \frac{1}{2\pi \mathrm{d}^2}\int_{-R_0}^{R_0} H(u)\Big(\int_{-\eta(\xi)}^{\eta(\xi)} I_s(\xi,\eta)\mathrm{d}\eta\Big)\mathrm{d}\xi \\ &= \frac{1}{2\pi \mathrm{d}^2}\frac{m}{M}\int_{\xi_0(x)}^{R_0} Y(\xi)\mathrm{d}\xi.\end{aligned} \tag{7}$$

The LSF is the derivate of the ESF

$$\frac{\mathrm{d}(\mathrm{ESF}(x))}{\mathrm{d}x} = \mathrm{LSF}(x). \tag{8}$$

For the source with Kapchiskij–Vladimirskij ($K-V$) distribution, $I_s(x,y) = 1/(\pi R_0^2)$. Let the new variable be $t = x/(MR_0)$, the equations of the LSF(x) and the ESF(x) are predigested and given by Eqs.(9) and (10), respectively. Figure 1 shows the curves of ESF(t) and LSF(t) when $R_0 = 2$ mm.

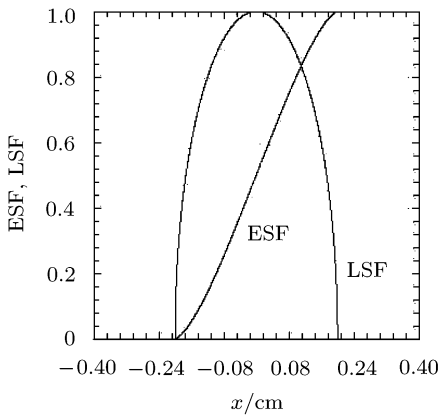


Fig.1. ESF and LSF curves of $K-V$ source.

$$E(t) = \begin{cases} 1, & (t \geq 1) \\ \dfrac{1}{2} + \dfrac{1}{\pi}t\sqrt{1-t^2} + \dfrac{1}{\pi}\sin^{-1}t, & (1 \geq t \geq -1) \\ 0, & (t \leq -1) \end{cases} \tag{9}$$

$$\mathrm{LSF} = \sqrt{1-t^2}\,. \tag{10}$$

4. The high-energy x-ray case

For the high-energy x-rays, the end side of the edge cell attenuates the x-rays which project on the corresponding zone. In order to examine the effect of cell thickness h on ESF and LSF, a few parameters are introduced (see Fig.2). These parameters are the effective source radius R_0, x-coordinates of the pixels x_1 and x_2, the path lengths of the x-rays across the end side of the cell $\ell_1(x,\xi)$ and $\ell_2(x,\xi)$, the conjugation source coordinates $\xi_1(x)$ and $\xi_2(x)$ of a pixel at x about the front corner and the back corner respectively. Obviously, $x_1 = M_1R_0$, $x_2 = M_2R_0$. Note that the path length, in the edge cell, of the x-rays emitted from the source with $\xi < 0$ to the pixel with $x > 0$ is $\ell_2(x,\xi)$, and the path length, in the edge cell, of the x-rays emitted from the source with $\xi > 0$ to the pixel with $x < 0$ is $\ell_1(x,\xi)$. The following equations are useful to obtain the ESF and LSF; because of $R_0 << h$ and $h << d$, the largest path length of x-rays in the edge cell is h approximately:

$$M_1 = \frac{L_2 + h/2}{L_1 - h/2}, \quad M_2 = \frac{L_2 - h/2}{L_1 + h/2}, \tag{11}$$

$$\ell_1(x,\xi) \approx L_1 + \frac{h}{2} - \frac{\mathrm{d}|\xi|}{|x| + |\xi|}, \tag{12}$$

$$\ell_2(x,\xi) \approx \frac{\mathrm{d}|\xi|}{|x| + |\xi|} - L_1 + \frac{h}{2}, \tag{13}$$

$$\xi_1(x) = -x/M_1, \quad \xi_2(x) = -x/M_2. \tag{14}$$

From Fig.2, it can be seen that the central line of the image can be divided into six zones, $x \geq x_1 \geq 0$, $x_1 \geq x \geq x_2 \geq 0$, $x_2 \geq x \geq 0$, $0 \geq x \geq -x_2$, $-x_2 \geq x \geq -x_1$, and $0 \geq -x_1 \geq x$. Obviously, the x-rays incident on the zone of $x \geq x_1 \geq 0$ is not decayed by the edge cell, but the transmissivity of any x-rays hitting at the zone of $0 \geq -x_1 \geq x$ is about $\exp(-\tilde{\mu}h)$. The x-rays arriving at other four zones will suffer more or less attenuation.

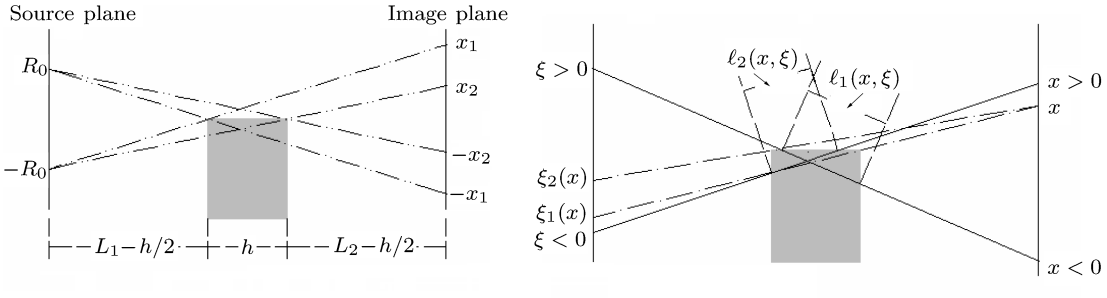


Fig.2. Geometry of the system.

$$\mathrm{ESF}(x) = \begin{cases} 1, & x > x_1; \\ \displaystyle\int_{-R_0}^{\xi_1(x)} Y(\xi)\exp[-\tilde{\mu}\ell_2(x,\xi)]\mathrm{d}\xi + \int_{\xi_1(x)}^{R_0} Y(\xi)\mathrm{d}\xi\,, & x_1 > x > x_2; \\ \mathrm{e}^{-\tilde{\mu}h}\displaystyle\int_{-R_0}^{\xi_2(x)} Y(\xi)\mathrm{d}\xi + \int_{\xi_2(x)}^{\xi_1(x)} Y(\xi)\exp[-\tilde{\mu}\ell_2(x,\xi)]\mathrm{d}\xi + \int_{\xi_1(x)}^{R_0} Y(\xi)\mathrm{d}\xi, & x_2 > x > 0; \\ \mathrm{e}^{-\tilde{\mu}h}\displaystyle\int_{-R_0}^{\xi_1(x)} Y(\xi)\mathrm{d}\xi + \int_{\xi_1(x)}^{\xi_2(x)} Y(\xi)\exp[-\tilde{\mu}\ell_1(x,\xi)]\mathrm{d}\xi + \int_{\xi_2(x)}^{R_0} Y(\xi)\mathrm{d}\xi, & 0 > x > -x_2; \\ \mathrm{e}^{-\mu h}\displaystyle\int_{-R_0}^{\xi_1(x)} Y(\xi)\mathrm{d}\xi + \int_{\xi_1(x)}^{R_0} Y(\xi)\exp[-\tilde{\mu}\ell_1(x,\xi)]\mathrm{d}\xi, & -x_2 > x > -x_1; \\ \mathrm{e}^{-\tilde{\mu}h}, & x < -x_1. \end{cases} \tag{15}$$

$$\mathrm{LSF}(x) = \begin{cases} 0, & x > x_1; \\ -\tilde{\mu}\mathrm{d}\displaystyle\int_{-R_0}^{\xi_1(x)} Y(\xi)\exp[-\tilde{\mu}\ell_2(x,-\xi)]\frac{\xi}{(\xi-x)^2}\mathrm{d}\xi, & x_1 > x > x_2; \\ -\tilde{\mu}\mathrm{d}\displaystyle\int_{\xi_2(x)}^{\xi_1(x)} Y(\xi)\exp[-\tilde{\mu}\ell_2(x,-\xi)]\frac{\xi}{(\xi-x)^2}\mathrm{d}\xi, & x_2 > x > 0; \\ \tilde{\mu}\mathrm{d}\displaystyle\int_{\xi_1(x)}^{\xi_2(x)} Y(\xi)\exp[-\tilde{\mu}\ell_1(x,-\xi)]\frac{\xi}{(\xi-x)^2}\mathrm{d}\xi, & 0 > x > -x_2; \\ \tilde{\mu}\mathrm{d}\displaystyle\int_{\xi_1(x)}^{R_0} Y(\xi)\exp[-\tilde{\mu}\ell_1(x,-\xi)]\frac{\xi}{(\xi-x)^2}\mathrm{d}\xi, & -x_2 > x - x_2; \\ 0, & x < -x_2. \end{cases} \tag{16}$$

According to Eqs.(1) and (4), the ESF(x) and the LSF(x) in the case of high-energy x-rays are given by Eqs.(15) and (16) respectively. The linear distribution function, $Y(\xi)$, of the x-ray sources with $K - V$

distribution is

$$Y(\xi) = \frac{2}{\pi R_0^2}\sqrt{R_0^2 - \xi^2}; \tag{17}$$

and for Gaussian (GS) case cut at $n\sigma$, $Y(\xi)$ is expressed as

$$Y(\xi) = \frac{1}{\sqrt{2\pi}\sigma(1-\exp(-n^2/2))} \times \operatorname{erf}\left(\sqrt{\frac{n^2}{2} - \frac{\xi^2}{2\sigma^2}}\right)\exp\left(-\frac{\xi^2}{2\sigma^2}\right). \tag{18}$$

Here σ is the variance of the GS distribution, $\operatorname{erf}(x)$ is the error function.

Figure 3(a) indicates the ESF profiles for the $K-V$ case, on the assumption of M=1, d=400 cm and R_0=2 mm, for the edge cell with different edge thickness (h). Figure 3(b) is the LSF distributions at different edge thicknesses of 2, 10 and 20 cm. The curve shift direction, when h increases, is shown with arrows. In Fig.3(a), with increasing h, the curve moves to the right with the centre point fixed. When the edge thickness increases, the added material of the cell near the image or the source makes x-rays further attenuated, so that the exposure on the detector reduces and the corresponding upper and lower parts of ESF curve (these parts marked with arrows in Fig.3(a)) all move towards the right direction.

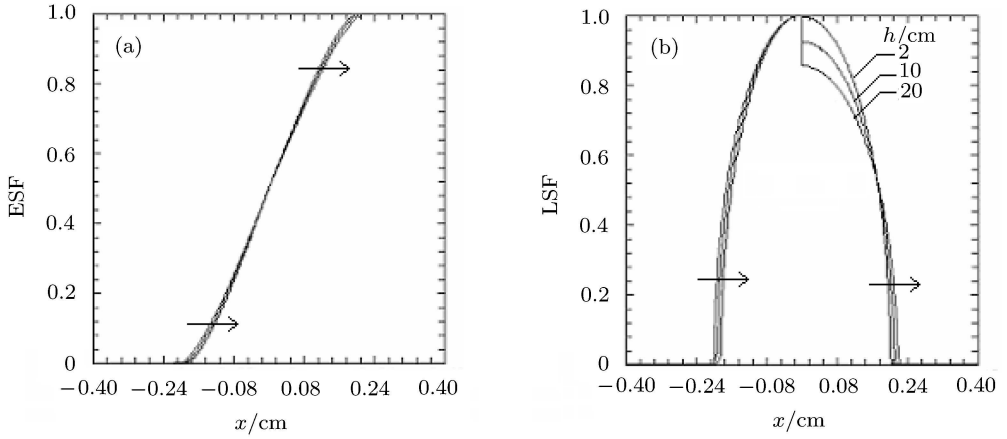


Fig.3. The curves of ESF (a) and LSF (b) in $K-V$ case for various h.

The LSF curve is interrupted at the projection point ($x = 0$) of the end side of the edge cell and the interrupted argument Δ becomes larger as h increases. With increasing h, the left part of the LSF curve becomes sharper and the right part wider. But, the width of the bottom of the LSF curve is almost the same for the case that the thickness is below 20 cm.

Figure 4(a) shows the numerical integration results of Eq.(16) for the GS case with the effective linear attenuation coefficient of 0.5 cm^{-1}. Figure 4(b) is the Monte Carlo simulation results with bremsstrahlung x-ray spectrum using the same parameters. Figure 4 shows that the results of Eq.(16) are in agreement with the Monte Carlo simulated results, and thus Eq.(16) is correct and reliable.

From the GS curve, it is shown that the trend of the effect of thickness h on the LSF curve is the same as that on the $K-V$ curve. It can be seen that the interrupted arguments are the same when the radiographic systems have the same edge thickness and are independent of the source intensity distribution and the sport size of the x-ray source. When the edge cell becomes thinner, for example $h < 6$ cm, the shape of LSF of the uniform intensity source is the elliptic style, and the shape of LSF of the source in the Gaussian case is the Gaussian style. To analyse the data of the LSF curve, it is found that the FWHM of LSF curve is equal to the FWHM of the intensity distribution of the x-ray source, and the relative error is less than 7%.

The interrupted argument Δ is defined as $\Delta \equiv \mathrm{LSF}(x \to 0_-) - \mathrm{LSF}(x \to 0_+)$. From Eq.(16), the expression is

$$\Delta \cong \mu \mathrm{d} Y(0) \mathrm{e}^{-\mu h/2}[\mathrm{e}^{\mu L_2}(E_1(z_1) - E_1(z_2)) + \mathrm{e}^{-\mu L_2}(E_\mathrm{i}(z_2) - E_\mathrm{i}(z_1))], \tag{19}$$

where both of $E_{\rm i}(x)$ and $E_1(x)$ are exponential integral functions[4,5]

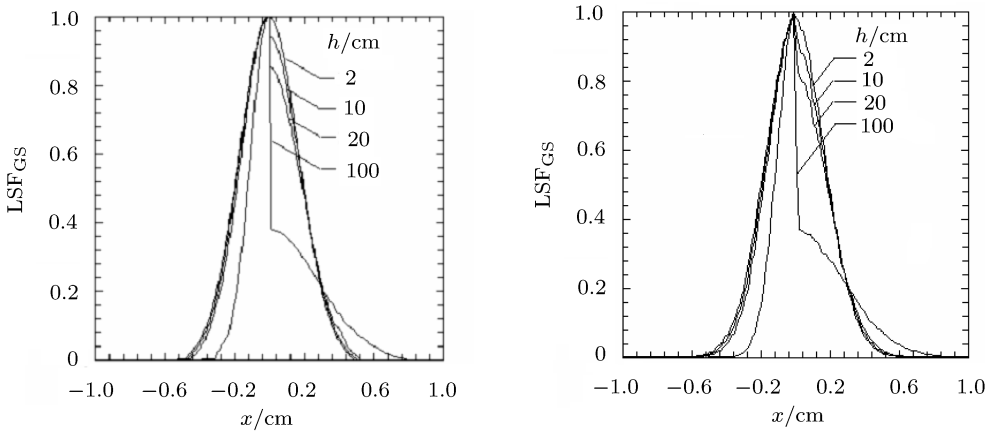
$$E_{\rm i}(x) = -\int_{-x}^{\infty} \frac{{\rm e}^{-t}}{t}{\rm d}t \quad (x > 0),$$

$$E_1(x) = \int_{x}^{\infty} \frac{{\rm e}^{-t}}{t}{\rm d}t \quad (x > 0),$$

and the arguments z_1 and z_2 are dependent on the radiographic layout and the effective attenuation coefficient of the material of edge cell.

$$z_1 = \frac{\tilde{\mu}d}{M_1 + 1}, \quad z_2 = \frac{\tilde{\mu}d}{M_2 + 1}.$$

In Eq.(19), $E_1(x)$ is a descending function, $E_{\rm i}(x)$ is an ascending function, and $z_2 > z_1$. Obviously, we have $\Delta > 0$. So LSF of the x-ray source of high energy is a discontinuous function at $x = 0$ with an interrupted argument Δ, and LSF $(x \to 0_-) >$ LSF$(x \to 0_+)$.



(a) Results of obtained using Eq.(16) (b) Monte Carlo simulation results

Fig.4. The curves of LSF for different edge thicknesses (a): $K - V$, (b): GS.

5. Monte Carlo simulation for the mismatching case

There are two mismatching cases, one is the cell end side being off the system axis, with a gentle shift in the x-direction ($x_{\rm off}$), another is the end side tilted from the axis, with a small tilt angle ($\theta_{\rm off}$). For the edge cell thickness of 10 cm, the radiographic images in both cases are simulated with the Monte Carlo method. The main purpose is to examine the effect of the two mismatching cases on the LSF curve and its FWHM.

For the shift case, the four systems with the shift from 0 to 3 millimetres by 1 millimetre increment are simulated. Figure 5 shows the resultant LSF curves, where the interrupted argument is decreased with increasing shift $x_{\rm off}$, and it shows that these LSF curves are similar in shape and size. For the tilt case, the four systems with the tilt angle ranging from 0 to 1.5 mrads by 0.5 mrad increment are simulated. Figure 6 shows the LSF curves, where the interrupted argument is fixed when the tilt angle $\theta_{\rm off}$ increases. Figure 6 also shows that there are little effects of small tilt angle on the shape and size of LSF curve.

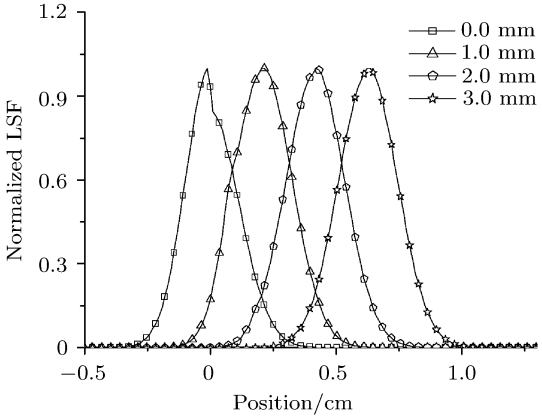


Fig.5. LSF curves with various shift $x_{\rm off}$.

The above results indicate that, for the less severely mismatching case, such as $x_{\rm off} < 3$ mm or

$\theta_{\text{off}} < 3$ mrad, the edge method is valid for measuring the spot size of the light source or the x-ray source.

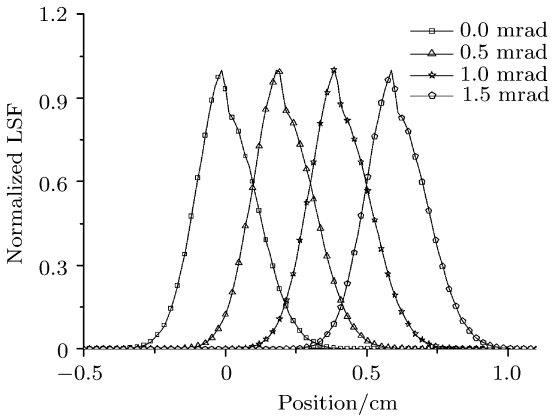


Fig.6. LSF curves with various tilt θ_{off}.

6. Conclusion

The edge method can be used directly to measure the spot size of the light source or the x-ray source with low or high energy. The basic procedure includes taking radiography with the edge cell, measuring ESF from the resultant image, obtaining the gradient curve LSF from the ESF curve, performing the Fourier transformation to present the modulation transfer function (MTF),[6] finding the frequency $f_{1/2}$ at MTF = 0.5, and finally providing the effective radius R_0 of x-ray source.

There is an interrupted argument Δ in the LSF curve of an x-ray source obtained with edge method at $x = 0$. The argument, Δ, given by Eq.(19), is proportional to the thickness of edge cell and is independent of the source intensity distribution and the sport size of the x-ray source. When the edge cell is thinner than 6 cm, the interrupted argument can be ignored. In experiment, it is appropriate to use the edge cell with a thickness of 6 cm.

In the mismatching case, where the cell end side is off the system axis or/and tilted from the axis, if mismatching extent is not serious, the edge method is valid for measuring the spot size of light source or the x-ray source.

References

[1] Kaftadjian V, Zhu Y M and Roziere G 1996 *J. X-ray Science and Technology* **6** 205

[2] Cao X, Huang H K and Lou S L 2000 *Proc. SPIE* **3977** 580

[3] Letang J M and Peix G 2003 *NDT & E International* **36** 303

[4] Abramowitz M and Stegun I A 1964 *Handbook of Mathematical Functions with Formulas, Graphs, and Mathematical Tables* (Washington, DC: US Government Printing Office) p228

[5] Writing group of Mathematics Handbook 1979 *Mathematics Handbook* (Beijing: Higher Education Publishing Company) p588 (in Chinese)

[6] Mueller K H 1989 LA-UR-89-1886